



Icariin mediates autophagy and apoptosis of hepatocellular carcinoma cells induced by the β -catenin signaling pathway through lncRNA LOXL1-AS1

Sicheng Gao¹ · Wanyi Zhang^{2,3} · Jinhua Dai¹ · Weiye Hu¹ · Yongyun Xu⁴ · Hailin Yang⁵ · Baiyang Ye¹ · Hao Ouyang¹ · Qinlin Tang¹ · Gang Zhao¹ · Junfeng Zhu¹

Received: 30 August 2024 / Accepted: 27 November 2024 / Published online: 15 January 2025
© The Author(s) 2025

Abstract

To investigate the effect of icariin (ICA) on hepatocellular carcinoma (HCC) and its autophagy/apoptosis mechanism in HCC. The anti-HCC mechanism of ICA was investigated using HCC cells treated with 20 $\mu\text{mol/L}$ ICA. Cell viability and proliferation were assessed using CCK-8 and colony formation assays, respectively, while TUNEL staining evaluated anti-apoptotic effects. DHE staining quantified intracellular ROS levels, and JC-1 staining assessed mitochondrial membrane potential. The expression of LC3 was detected by immunofluorescence staining. Additionally, HepG2 cells (2.0×10^6) were implanted into the thymus of BALB/c nude mice, which received intraperitoneal injections of 40 mg/kg ICA. Western blotting was used to evaluate the expression of proteins related to apoptosis and autophagy. ICA effectively inhibited the proliferation and invasion of HCC cells, enhancing autophagy and apoptosis. Silencing of lncRNA *LOXL1-AS1* reduced β -catenin expression and downregulated PI3K/AKT/mTOR pathway phosphorylation. Targeting β -catenin with siRNA augmented apoptosis in HepG2 cells through elevated levels of Bax and caspase-3/8/9 and boosted autophagy via increased expression of LC3-II, Atg5, Atg7, Atg8, and Beclin-1. ICA reversed this autophagic effect, while rapamycin enhanced ICA's efficacy. In vivo, ICA suppressed tumor growth and promoted autophagy and apoptosis in mice. Icariin induces autophagy and apoptosis in HCC cells via the β -catenin signaling pathway mediated by lncRNA *LOXL1-AS1*, offering a novel approach to HCC clinical management.

Keywords Icariin · lncRNA *LOXL1-AS1* · Hepatocellular carcinoma · β -catenin · Autophagy · Apoptosis

Introduction

Hepatocyte apoptosis is a key pathological feature of HCC, and targeting this may help disease progression (Wang 2015). However, no specific clinical treatment currently target this pathway, and its underlying mechanisms remain under investigation (Wang 2014). Autophagy is a complex mechanism that transfer cellular materials to

lysosomes for degradation (Wu et al. 2021) and plays a dual role in liver cancer, both suppressing and promoting tumor growth. The modulation of autophagy can influence liver cancer outcomes by either enhancing or diminishing prognosis (Liu et al. 2017). For instance, the resistance of HCC to sorafenib is linked to autophagy, which sustains tumor viability by promoting drug resistance, while excessive autophagy might suppress apoptosis (Li et al. 2018; Liu et al. 2017; Wu et al. 2021). Strategies that regulate apoptosis to curb excessive autophagy could enhance therapeutic efficacy (Spirina et al. 2020; Tompkins and Thorburn 2019). Activation of the Wnt/ β -catenin signaling pathway has been reported to reduce Beclin-1 expression and autophagy in tumor cells, thereby increasing apoptosis (Nguyen et al. 2009). While autophagy and apoptosis are distinct processes that similar upstream signals can initiate, their interplay remains poorly understood in HCC (Sun et al. 2020). Exploring the crosstalk and bidirectional interactions between autophagy and apoptosis could open

Sicheng Gao, Wanyi Zhang, and Jinhua Dai shared equal contributions.

Highlights

- The ICA affects the treatment of hepatocellular carcinoma.
- ICA can promote cell autophagy and apoptosis of liver cancer.
- lncRNA *LOXL1-AS1* regulates β -catenin expression and PI3K/AKT/mTOR phosphorylation.
- Silence β -catenin autophagy induced liver cancer cells.

Extended author information available on the last page of the article

new therapeutic avenues for HCC treatment (Niu et al. 2020).

ICA, the primary active component of the Chinese herb *Epimedium* (Li et al. 2021), has been widely recognized for its regulatory effects on cancer, particularly in HCC (Li et al. 2020a, b; Mo et al. 2021; Wang et al. 2020; Li et al. 2021; Yu et al. 2020). It has been shown to modulate immune responses by reducing T lymphocyte subsets and enhancing the production of inflammatory markers, key factors in HCC prognosis (Qin et al. 2020). In addition, ICA can also inhibit the invasion and metastasis of tumor cells and prolong the survival time of patients with advanced HCC by inducing apoptosis (Algandaby et al. 2017; Bailly 2020; Chen et al. 2019; Qin et al. 2020; Tang et al. 2015; Wang 2014; Yang et al. 2017). The bidirectional regulation of ICA is also reflected in autophagy. Recent studies have found that ICA plays a role in anti-autophagy (Algandaby et al. 2017) and can also induce autophagy (Yang et al. 2019). Several in vitro experiments highlight ICA's role in the crosstalk between autophagy and apoptosis, enhancing apoptosis through autophagy inhibition (Bailly 2020; Jiang et al. 2018; Tang et al. 2015). Nevertheless, its specific function in autophagy and apoptosis within HCC remains to be fully elucidated. Autophagy can induce apoptosis and inhibit apoptosis (Sun et al. 2020). The precise role of ICA in these processes, particularly through bidirectional autophagy, remains a key question.

lncRNA, consisting of over 200 nucleotides, plays crucial roles in regulating tumor cell proliferation, differentiation, autophagy, and apoptosis (Huang et al. 2020a, b; Yu and Dai 2021). It primarily influences cellular processes by interacting with miRNAs (ceRNA hypothesis) (Xie et al. 2019) and forming lncRNA-protein complexes (Kazimierczyk et al. 2020). Various lncRNAs have been confirmed to induce autophagy in HCC. For instance, lncRNA HNF1A-AS1, lncRNA CCAT1, lncRNA HCG11, and lncRNA LINC00665 can stimulate autophagy by regulating the expression of *ATG5*, *ATG7*, *ATG12*, and *MAP4K3* in HCC, respectively (Guo et al. 2019; Li et al. 2019a, b; Liu et al. 2016; Shan and Li 2019). LOXL1-AS1 is located on human chromosome 15Q24.1, consisting of 10781 nucleotides and five exons (Sun et al. 2019). Studies have confirmed that LOXL1-AS1 plays a carcinogenic role in a variety of human cancers, such as HCC (Yu and Dai 2021), lung adenocarcinoma (Li et al. 2020a, b), non-small-cell lung cancer (Xie et al. 2019), medulloblastoma (Gao et al. 2018), and breast cancer (Li et al. 2019a, b). Recent findings suggest that LOXL1-AS1 promotes glucose metabolism, proliferation, migration, and epithelial-mesenchymal transition of HCC by targeting miR-377-3p/NFIB (Xie et al. 2019). However, the role of LOXL1-AS1 in the autophagy and apoptosis of HCC remains unexplored.

The nuclear accumulation of β -catenin plays a carcinogenic role in HCC (Cordenonsi et al. 2011), promoting unrestricted cell proliferation, invasion, and metastasis. Our previous studies found that O-GlcNAc-mediated β -catenin glycosylation induces proliferation and invasion, thereby inducing apoptosis of HCC cells (Gao et al. 2019). Additionally, it has been observed that activation of the Wnt/ β -catenin signaling pathway reduces autophagy while increasing apoptosis in tumor cells (Huang et al. 2020a, b; Nguyen et al. 2009). Therefore, investigating the role of β -catenin in HCC is crucial.

In this study, we aim to investigate how ICA may regulate the autophagy/apoptosis of HCC cells induced by *LOXL1* through β -catenin. We first measured ICA activity, proliferation, invasion, and apoptosis of HCC cells. ROS production and mitochondrial membrane potential of HepG2 and Bel-7402 cells were measured to evaluate ICA's effect on HCC cell apoptosis. TEM and 3-MA were used to evaluate the autophagy of ICA in HepG2 cells. qRT-PCR evaluated whether ICA activated *LOXL1-AS1*/ β -catenin signaling in HepG2 cells. Knocking down *LOXL1-AS1* and β -catenin was to explore the mechanism of autophagy and apoptosis. Finally, the apoptosis/autophagy effects of ICA were verified by the xenograft tumor model in vivo.

Methods and materials

Cell culture and reagents (Sun et al. 2020; Zhou et al. 2017)

The HepG2 cells (American Type Culture Collection) and Bel-7402 cells were cultured in ATCC-formulated Eagle's Minimum Essential Medium (EMEM, Gibco) supplemented with 10% fetal bovine serum (FBS, Gibco), penicillin (100 units/mL, Gibco), and streptomycin (100 g/mL, Gibco). The cell lines were incubated with 5% CO₂ at 37 °C. ICA with a purity of 99% was obtained from Selleck and dissolved in DMSO (concentration 1 mg/mL) at various concentrations (2.5, 5, 10, 20, and 40 mM) and stored at −20 °C. The medium was changed to phenol red-free medium with 10% FBS before ICA was added. All cells were confirmed to be negative for mycoplasma by Mycoplasma Detection Kit (Solarbio, Beijing, China). Autophagy inhibitors 3-methyladenine (3-MA) and agonists rapamycin were obtained from Sigma-Aldrich (St. Louis, MO).

In our initial experiments, we employed both Bel-7402 and HepG2 cells to establish a broader understanding of ICA's effects across different HCC models. Bel-7402 cells were specifically used in early experiments to validate the reproducibility of HepG2 findings and to ensure that the observed effects were not cell line-specific. After preliminary experiments, we focused on HepG2 cells for detailed

investigation due to their consistent response profiles and extensive characterization in literature, which supports their relevance for elucidating the molecular mechanisms underpinning HCC responses to treatment.

Cell transfection assay

The siRNAs targeting β -catenin and *LOXLI-AS1* were designed and synthesized by RiboBio (Guangzhou, China). The sequences for *LOXLI-AS1*-targeting siRNA (si LOXLI-AS1) were 5'-GCUCAGUCUUACUAAUAAAGG-3' (sense) and 5'-UUUAUUAGUAAGACUGAGCAC-3' (antisense). For β -catenin-targeting siRNA (si β -catenin), the sequences were 5'-GCUCAGUCUUACUAAUAAAGG-3' (sense) and 5'-UUUAUUAGUAAGACUGAGCAC-3' (antisense). The plasmid and siRNAs were transfected into HepG2 cells using Lipofectamine 3000 (L3000150, Thermo Fisher Scientific, USA) according to the manufacturer's instructions [41]. The HepG2 cells were divided into 7 groups: PBS (phosphate buffer saline) (control), ICA (20 μ mol/L), ICA (20 μ mol/L) + 3-methyladenine (3-MA, 1.0 mM), 3-methyladenine (3-MA, 1.0 mM), si- β -catenin (100 μ mol/L), si- β -catenin (100 μ mol/L) + ICA (20 μ mol/L), si- β -catenin (100 μ mol/L) + rapamycin (100 nmol/L) + ICA (20 μ mol/L), si-LOXLI-AS1 (100 μ mol/L), si- β -catenin (100 μ mol/L). The Bel-7402 cells were divided into 2 groups: PBS (phosphate buffer saline) (control) and ICA (20 μ mol/L). Cells in all groups were harvested after 48 h to measure the expression of corresponding cellular markers.

Cell growth assay (Sun et al. 2020)

Cell proliferation was evaluated using the Cell Counting Kit-8 (CCK-8) assay. Cells were isolated and seeded in a complete growth medium at a density of 1.5×10^3 cells. HepG2 and Bel-7402 cells were pretreated with PBS, 20 μ mol/L ICA, 1.0 mM 3-MA, and ICA (50 μ mol/L) + 3-MA (1.0 mM) for 48 h. Subsequently, the 96-well plates were placed in an incubator at 37 °C with 5% CO₂. CCK-8 assay was performed according to the manufacturer's instructions. Absorbance at 490 nm was obtained by a microplate reader (BioTek Instruments, Inc).

Colony formation assay (Sun et al. 2020)

HepG2 and Bel-7402 cells were pretreated with PBS and 20 μ mol/L ICA. Cells were cultured in a drug-free medium for approximately 14 days. The cells were fixed with cold methanol-glacial acetic acid and stained with crystal violet for 4 h. Finally, the staining results were observed under an inverted microscope at $\times 100$ magnification (Tokyo, Japan).

Cell invasion assay and cell scratch assay (Sun et al. 2020)

A Transwell assay was performed to detect cell invasion in HepG2 and Bel-7402 cells. HepG2 and Bel-7402 cells were seeded (5×10^4 cells/200 μ L) into the upper Transwell chamber with serum-free DMEM. The lower chamber was filled with 500 μ L EMEM containing 10% FBS. Simultaneously, PBS (control) or 20 μ mol/L ICA was added into the upper chamber. After a 24-h incubation, cells in lower chambers were fixed in 95% ethanol and stained with hematoxylin. The invasive number of cells was calculated and imaged under an inverted microscope at $\times 400$ magnification (Tokyo, Japan). For cell scratch assay, 5×10^5 cells were scraped in a 6-well plate using a sterile pipette for a gap of about 1 mm. HepG2 and Bel-7402 cells were pretreated with PBS, 20 μ mol/L ICA at 37 °C for 24 h. Cell images in the scratch area were captured under an inverted microscope at $\times 100$ magnification (Tokyo, Japan).

Cell apoptosis assay (Li et al. 2021; Ni et al. 2020; Sun et al. 2020)

TUNEL staining was performed to detect cell apoptosis. HepG2 cells treated with ICA for 24 hours were processed using a TUNEL assay kit (Roche Applied Science, Indianapolis, in the USA) at 37 °C for 60 min and at 18–25 °C for 15 min with DAPI-Fluoromount-G. Fluorescence was evaluated using an inverted microscope (Eclipse Ti-U, Nikon, Japan) with an excitation range of 450–500 nm and detection at 515–565 nm (green) and 358–461 nm (blue). The number of TUNEL-positive cells and the DAPI-stained nuclei was determined and repeated at least 3 times. To avoid bias and ensure that all results were reliable, counting was anonymously conducted by two independent individuals (Ferretti et al. 2019).

Dihydroethidium (DHE) staining

DHE staining was employed to assess intracellular levels of superoxide anions, serving as an indicator of ROS. Cells were seeded at a density of 7500 cells per well in a black 96-well plate with a clear bottom and incubated at 37 °C for 24 h to allow attachment. After 24 h incubation, the medium was replaced with one containing previously specified concentrations of various substances. Subsequently, the medium was with a 10 μ M fluorescent probe (DHE 100 μ L/well). The probe stock solution was prepared in DMSO, and the working solution was prepared in PBS. Fluorescence was measured at a wavelength of 475/579 nm (DHE) at 1-min intervals for 2 h (Pieńkowska et al. 2021).

JC-1 staining

JC-1 staining was used to measure the mitochondrial membrane potential. The cells were stained with 2.5 mmol/L JC-1 staining solution for 30 min at 37 °C in the dark. The images were obtained using fluorescence microscopy (Tokyo, Japan) at $\times 400$ magnification.

Cellautophagy assay (Sun et al. 2020)

The position of LC3 was detected by immunofluorescence staining. MRFP-GFP-LC3 adenovirus (Hanbio, China) was transfected into liver cancer cells for 24 h, followed by treatment with 20 μ mol/L ICA for 48 h. Cells were then fixed in 4% paraformaldehyde and examined under a confocal microscope (Leica, Germany) to observe LC3 staining. The GFP-positive/mRFP-positive (yellow) and GFP-negative / mRFP-positive (red) spots in cells were counted by confocal to evaluate autophagy flux. The experiment was repeated thrice, and each group counted 50–100 cells (Zhou et al. 2019).

Western blot

Cells and tumor tissues were lysed using ice-cold RIPA buffer with protease inhibitors. Protein concentrations were determined colorimetrically using bicinchoninic acid protein dye reagent (Pierce, Thermo Fisher Scientific, Inc., Waltham, MA, USA). Proteins were separated using SDS-PAGE and transferred to polyvinylidene difluoride (PVDF) membranes. The membranes were blocked with 5% BSA in TBST and incubated with primary antibodies sourced from Abcam: anti-PI3K, AKT and mTOR (Abcam), anti-GAPDH (Abcam), anti-Ki67 (Abcam), anti-caspase-3,8,9 (Abcam), anti-VEGF (Abcam), anti-MMP-9 (Abcam), anti-cleaved caspase-3,9, anti- β -catenin, anti-Bcl-2, anti-Bcl-XL, anti-Bax, anti-LC3-II/LC3-I, anti-Atg5, anti-Atg7, anti-Atg8, anti-Beclin-1, and anti-p62. After washing, the membranes were incubated with horseradish peroxidase (HRP)-conjugated secondary antibody (Santa Cruz Biotechnology). The target proteins were visualized using the Amersham ECL Prime Western Blotting Detection Reagent (Amersham Pharmacia Biotech). Finally, protein images were obtained by a ChemiDoc XRS imaging system and analyzed by Quantity One analysis software (Bio-Rad Laboratories).

Quantificational real-Time PCR Analysis (Deng et al. 2018)

The expression of β -catenin and *LOXL1-AS1* was quantified using quantitative real-time PCR (qRT-PCR) on the CFX96 Real-Time System (Bio-Rad, USA). Sangon Biotech (Shanghai, China) provided the primers, and *GAPDH*/U6 was used

as the internal reference. The following primers were used: β -catenin forward: 5'-CTCCAAGAATGGAGGCTGTAG GAA-3', reverse: 5'-CCTATGAGATGGAGCAGGCAAGA-3'; *LOXL1-AS1* forward: 5'-TTCCCATTTACCTGCCCCG AAG-3', reverse: 5'-GTCAGCAAACACATGGCAAC-3'; and *GAPDH* forward: 5'-CTGGGCTACACTGAGCACC-3', reverse: 5'-AAGTGGTCGTTGAGGGCAATG-3'. Data were analyzed using the comparative Ct ($2^{-\Delta\Delta C_t}$) method.

The xenograft tumor model assay

Six-week-old female BALB/c thymus nude mice were used to establish an orthotopic xenograft mouse model, and HepG2 cells (2.0×10^6) were inoculated on the right side near the hind legs of each nude mouse. The model mice were divided into a control group (saline injection) and an ICA group (40 mg/kg ICA injection), with 6 mice in each group. Mice in the ICA group received intraperitoneal injections of 40 mg/kg ICA three times a week on the first day after the injection of tumor cells. All animals were killed on the 30th day, and the median survival time and tumor weight were measured (Huang et al. 2020a, b).

Immunohistochemistry assay

Mouse tumor tissues were fixed in a 4% neutral formaldehyde solution, dehydrated with gradient alcohol, transparent with xylene, embedded in paraffin, and sliced into 4- μ m-thick sections. For antigen retrieval, sections were treated with EDTA (pH 8.0) in a composite-bottom aluminum pressure cooker. The sections were then blocked for endogenous peroxidase activity with 3% hydrogen peroxide at room temperature for 10 min, followed by three washes in PBS for 5 min each. Subsequently, sections were incubated with primary antibodies against Ki67 and VEGF (Abcam) at room temperature (25 °C) for 2 h, followed by three PBS washes of 2 min each. Secondary antibodies were applied for 30 min at 25 °C and then washed off similarly. DAB was added to the tissue for 10 min. After hematoxylin counterstaining for 1 min and gradient ethanol dehydration, xylene was added, and the slides were sealed with neutral gum. Finally, the staining results were observed under an inverted microscope at $\times 100$ magnification (Tokyo, Japan) (Nahari et al. 2007).

Statistics analysis (Sun et al. 2020)

SPSS software (version 19.0) was used for all the statistical analyses. The data were presented as mean \pm SD. Statistical comparisons were analyzed by one-way analysis of variance (ANOVA) followed by the least significant difference (LSD) test. The difference was considered statistically significant when values of $P < 0.05$.

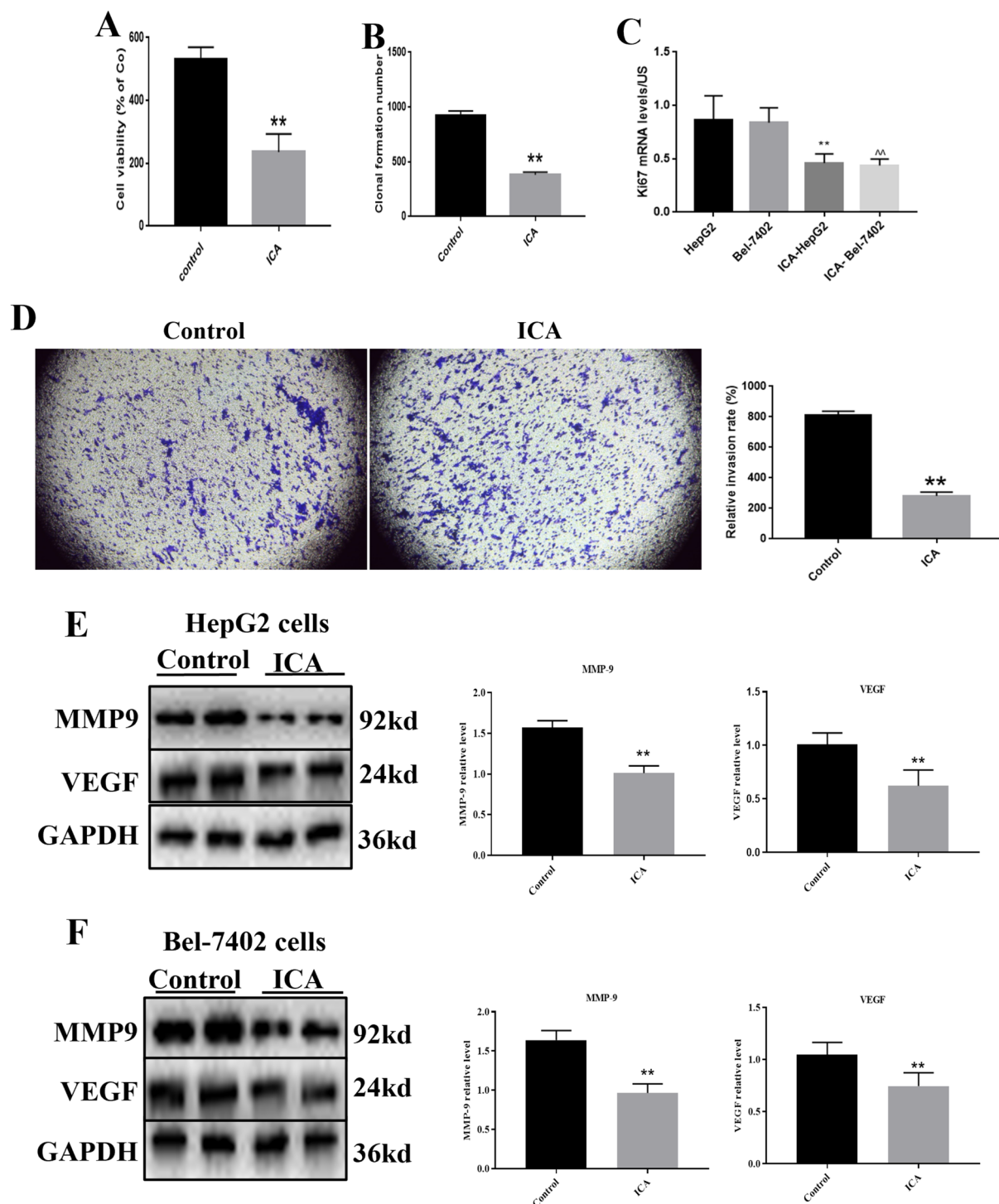


Fig. 1 ICA inhibited cell proliferation and invasion in the 20 $\mu\text{mol/L}$ ICA-treated group or the control group. **A** The viability of HepG2 cells was analyzed using a CCK-8 assay. **B** The colony formation ability of HepG2 cells was determined. **C** qRT-PCR was used to detect mRNA expression of Ki67 in HepG2 cells and Bel-7402 cells. **D** The invasion of HepG2 cells was analyzed by Transwell assay (magnification, $\times 200$). **E** The expressions of MMP-9 and VEGF of HepG2 cells were detected by Western blotting. GAPDH was used as

a control substance, and the representative column diagrams showed results of relative protein expression. **F** The expressions of MMP-9 and VEGF of Bel-7402 cells were detected by Western blotting. GAPDH was used as a control substance, and the representative column diagrams showed results of relative protein expression. Data was represented as the mean \pm SD of three independent experiments. ** $P < 0.01$ vs. control

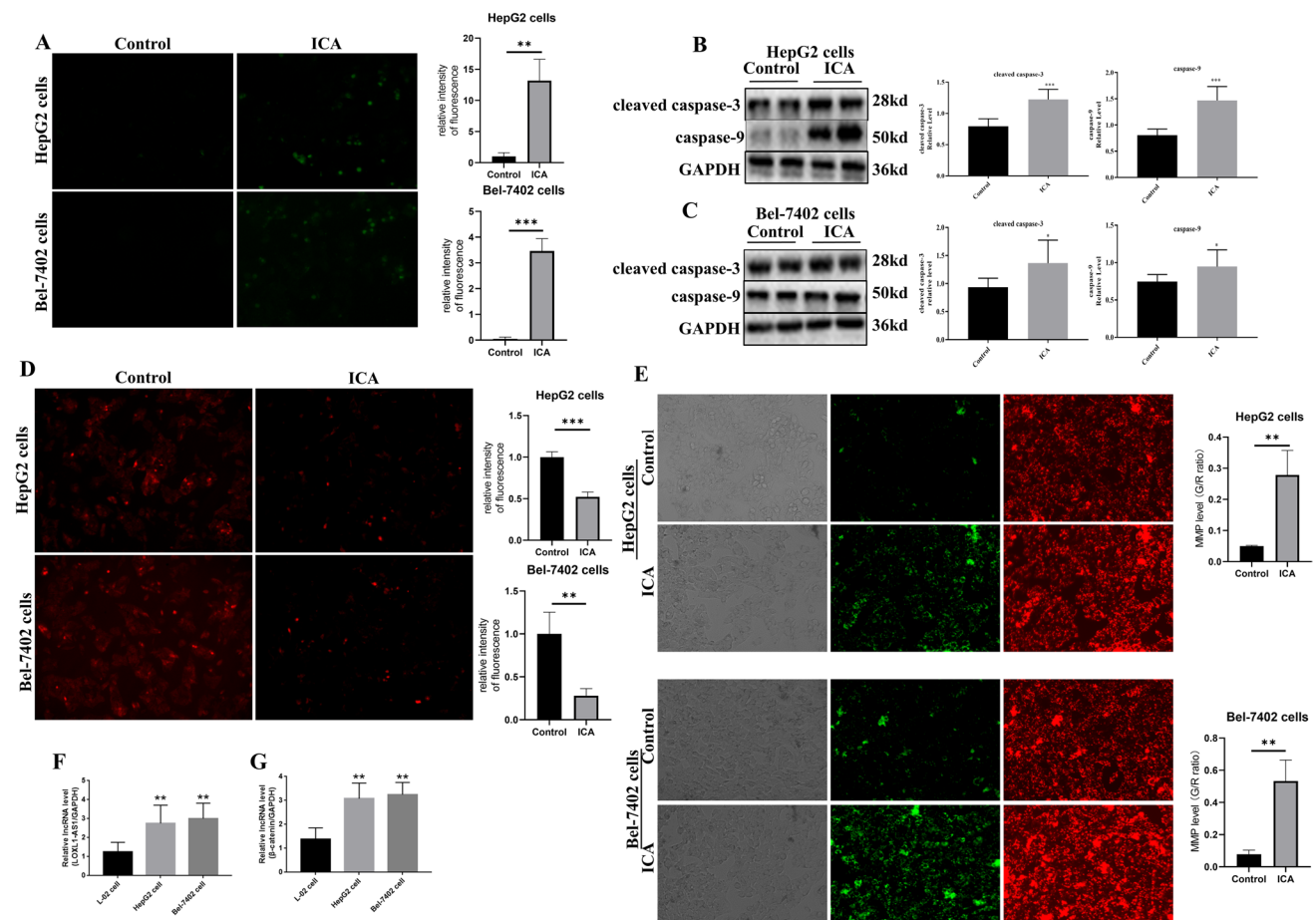


Fig. 2 ICA promoted apoptosis of HepG2 cells and Bel-7402 cells in the 20 $\mu\text{mol/L}$ ICA-treated group compared with the control group. **A** Cell apoptosis was detected by TUNEL staining. **B** Protein expression of cleaved caspase-3 and caspase-9 HepG2 cells was detected by Western blotting, and the representative column diagrams show results of relative protein expression. **C** Protein expression of cleaved caspase-3 and caspase-9 of Bel-7402 cells was detected by Western blotting, and the representative column diagrams show results of relative protein expression. **D** Intracellular levels of superoxide anions in

the cells to access the level of ROS were detected by DHE staining. **E** JC-1 staining measured the mitochondrial membrane potential, magnification $\times 400$. **F** qRT-PCR was performed to assess the relative IncRNA level of LOXL1-AS1 in HepG2 cells, Bel-7402 cells, and L-02 groups. **G** qRT-PCR performed the relative IncRNA level of β -catenin in HepG2 cells, Bel-7402 cells, and L-02 groups. Data was represented as the mean \pm SD of three independent experiments. $^{**}P < 0.01$ vs. control; $^{**}P < 0.01$ vs. L-02 cell

Results

ICA inhibited cell proliferation and invasion in vitro

The effect of ICA on viability and proliferation in HepG2 was confirmed by CCK-8 (Fig. 1A) and colony formation (Fig. 1B). Compared with the control group, ICA treatment significantly inhibited the viability and proliferation of HepG2 cells ($p < 0.01$). The mRNA expression of Ki67 was significantly inhibited in the ICA-treated HepG2 and Bel-7402 cells group (Fig. 1C). The inhibitory effect of ICA on cell invasion was demonstrated using a Transwell assay, which showed a significant reduction in the invasive capacity of HepG2 cells (Fig. 1D, $p < 0.01$). The relative expressions of MMP-9 and VEGF were decreased significantly in

HepG2 and Bel-7402 cells treated with ICA (Fig. 1E, F). It followed that ICA inhibited cell proliferation and invasion in vitro.

ICA promoted cell apoptosis in vitro

Further investigations confirmed that ICA could induce apoptosis in HCC cells. TUNEL staining (Fig. 2A) demonstrated increased apoptosis in HepG2 and Bel-7402 cells following ICA treatment compared to controls. The relative expressions of cleaved caspase-3 and caspase-9 were increased significantly in HepG2 and Bel-7402 cells treated with ICA groups (Fig. 2B, C, $p < 0.05$). In addition, ICA significantly reduced the production of ROS in the cell

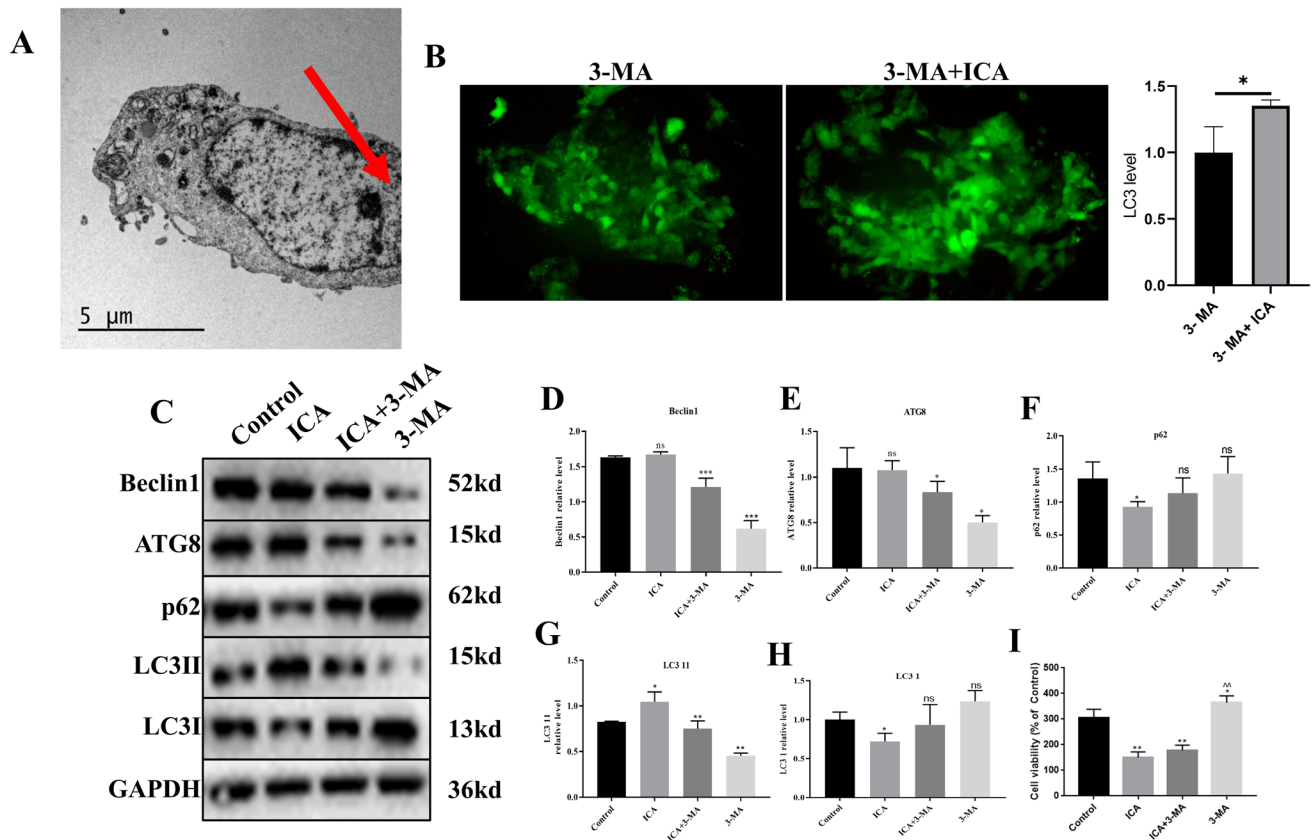


Fig. 3 ICA-induced autophagy of HCC cells. **A** Representative images of intracellular double-membrane vesicles, the ultrastructural feature of autophagy, detected by TEM in the 20 $\mu\text{mol/L}$ ICA-treated group. **B** LC3 (green) in HepG2 cells was detected by immunofluorescence assay. DAPI (blue) = nuclei. **C** The protein expression of autophagy-related markers (Beclin-1, ATG8, p62, LC3II/LC3I) was detected by Western blotting in HepG2 cells (20 $\mu\text{mol/L}$ ICA for 24

h). **D–H** The representative column diagrams showed results of relative protein expression. **I** HepG2 cells were treated with ICA, ICA (20 $\mu\text{mol/L}$) + autophagy inhibitors: 3-methyladenine (3-MA, 1.0 mM), 3-MA, (1.0 mM) for 24 h. Cell viability was determined by CCK-8 assay. Data was represented as the mean \pm SD of three independent experiments. * $P < 0.05$, ** $P < 0.01$ vs. control, *** $P < 0.01$ vs. ICA + 3-MA

membrane (Fig. 2D). The JC-1 findings confirmed that the ICA intervention could reduce the transmembrane potential of mitochondria, as revealed by the transition from red to green JC-1 fluorescence (Fig. 2E). The results revealed that ICA could induce apoptosis of hepatoma cells.

ICA promoted cell apoptosis via the LOXL1-AS1/ β -catenin axis in vitro

To explore ICA impact on apoptosis by regulating the LOXL1-AS1/ β -catenin axis, we performed qRT-PCR assays for *LOXL1-AS1* and β -catenin in HCC cells and human normal hepatocytes L-02 (ATCC). Our findings indicated higher expression of *LOXL1-AS1* in HCC cells compared to L-02 cells (Fig. 2F), with β -catenin showing a similar pattern (Fig. 2G). These results suggest that ICA can promote apoptosis by targeting the LOXL1-AS1/ β -catenin axis.

ICA-induced autophagy in HCC cells

We observed the activation of autophagy by TEM to further clarify the effect of ICA on autophagy. Findings revealed an increased number of dual-membrane structures resembling autophagosomes in HepG2 cells treated with ICA (Fig. 3A). Then, ICA-induced cell autophagy was blocked by 3-MA treatment. In the blank control group, diffusely distributed mRFP and GFP signals were detected, indicative of LC3 dispersion. Twenty-four hours after ICA application, yellow and red spots were observed in the perinuclear region, suggesting the formation of early autophagosomes. The combination of 3-MA + ICA blocked the autophagy flux induced by ICA. Moreover, the number of mRFP-GFP-LC3 spots in the 3-MA + ICA group was significantly decreased as compared with the 3-MA group (Fig. 3B). Western blot analysis revealed increased levels of LC3-II and Beclin-1 and decreased levels of p62 and LC3-I in cells treated with ICA,

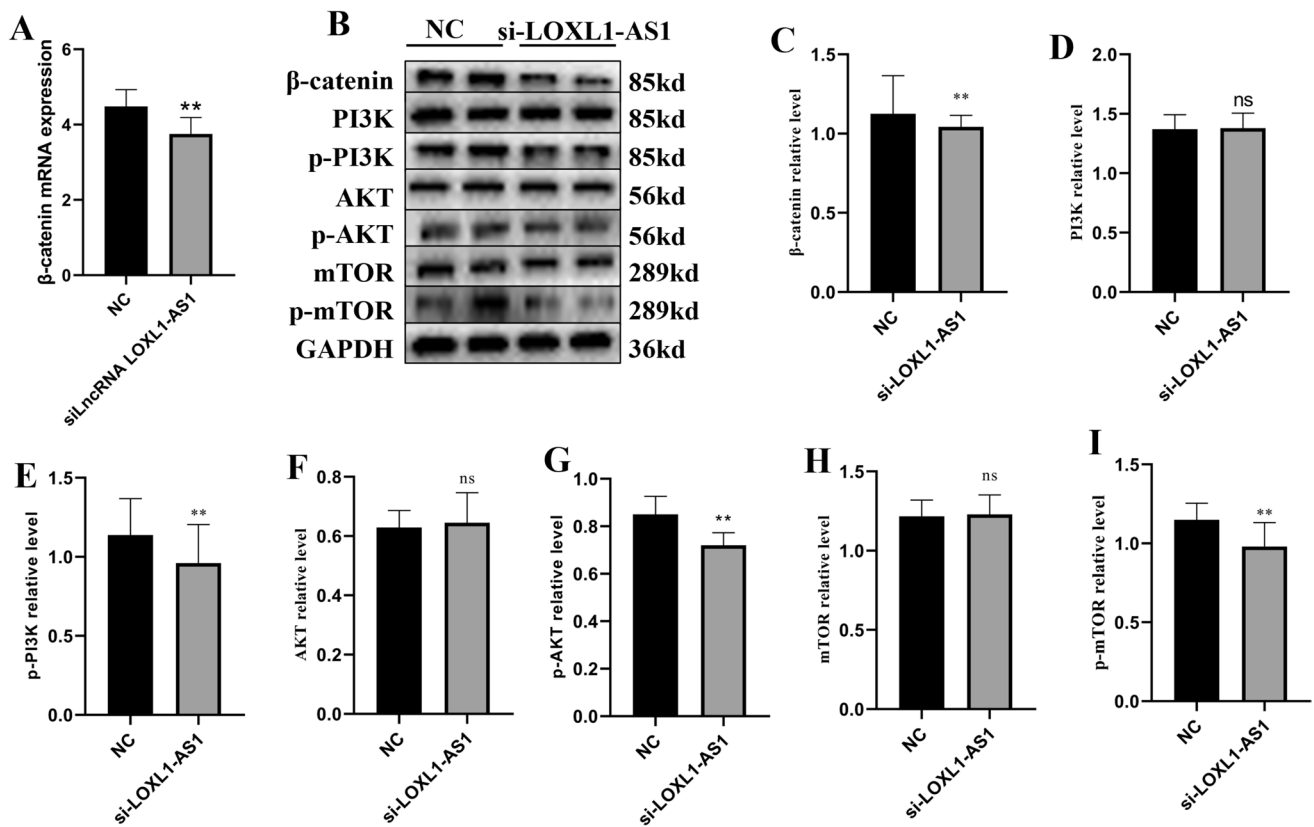


Fig. 4 Silencing lncRNA *LOXL1-AS1* inhibited β -catenin expression and PI3K/AKT/mTOR phosphorylation of HepG2 cells. **A** qRT-PCR analyzed the expression level of β -catenin. **B** Protein expression of β -catenin, PI3K, p-PI3K, AKT, p-AKT, mTOR, and p-mTOR was analyzed by Western blotting. **C–I** The representative column dia-

grams showed results of relative protein expression of β -catenin, PI3K, p-PI3K, AKT, p-AKT, mTOR, and p-mTOR. Data was represented as the mean \pm SD of three independent experiments. ** $P < 0.01$ vs. NC; ns means no significant difference

confirming autophagy induction (Fig. 3C–H, $p < 0.05$). The addition of 3-MA reversed ICA's inhibitory effects on HCC cell proliferation as measured by the CCK-8 assay (Fig. 3I), further validating that ICA induces autophagy in HCC cells.

Silencing lncRNA *LOXL1-AS1* inhibited β -catenin expression and PI3K/AKT/mTOR phosphorylation

Activation of the Wnt/ β -catenin signaling pathway reduces Beclin-1 expression, diminishes autophagy, and increases apoptosis in tumor cells (Nguyen et al. 2009). β -catenin, a pivotal protein in the Wnt/ β -catenin signaling pathway, plays a crucial regulatory role in several physiological processes, including embryonic development, cell differentiation, proliferation, movement, adhesion, and apoptosis (Chen et al. 2020). Additionally, it is implicated in various stages of tumorigenesis. To further explore the relationship between *LOXL1-AS1* and β -catenin, the expression of β -catenin of HepG2 cells transfected with si-*LOXL1-AS1* was detected by qRT-PCR, and the result showed that si-*LOXL1-AS1* could inhibit β -catenin in HepG2 cells (Fig. 4A). The expression

of β -catenin, PI3K, p-PI3K, AKT, p-AKT, mTOR, and p-mTOR of HepG2 cells transfected with si-*LOXL1-AS1* was detected by Western blot, and we found that the expressions of β -catenin, p-PI3K, p-AKT, and p-mTOR in HepG2 cells were inhibited by si-*LOXL1-AS1* (Fig. 4B–I). These findings suggest that lncRNA *LOXL1-AS1* regulates β -catenin expression and PI3K/AKT/mTOR phosphorylation in HepG2 cells.

Silencing lncRNA β -catenin promoted apoptotic of HepG2 cells

To examine the effect of lncRNA β -catenin on the apoptosis of HepG2 cells, cells were transfected with a β -catenin silencing construct. TUNEL staining confirmed significant induction of apoptosis following β -catenin knockout (Fig. 5A). In si- β -catenin-treated HepG2 cells, the expression of apoptosis-related proteins Bcl-2, Bcl-XL, Bax, and caspase-3/8/9 was detected by Western blot (Fig. 5B–H). We found that the expression of Bcl-2 and Bcl-XL was significantly downregulated, and the expression of Bax and

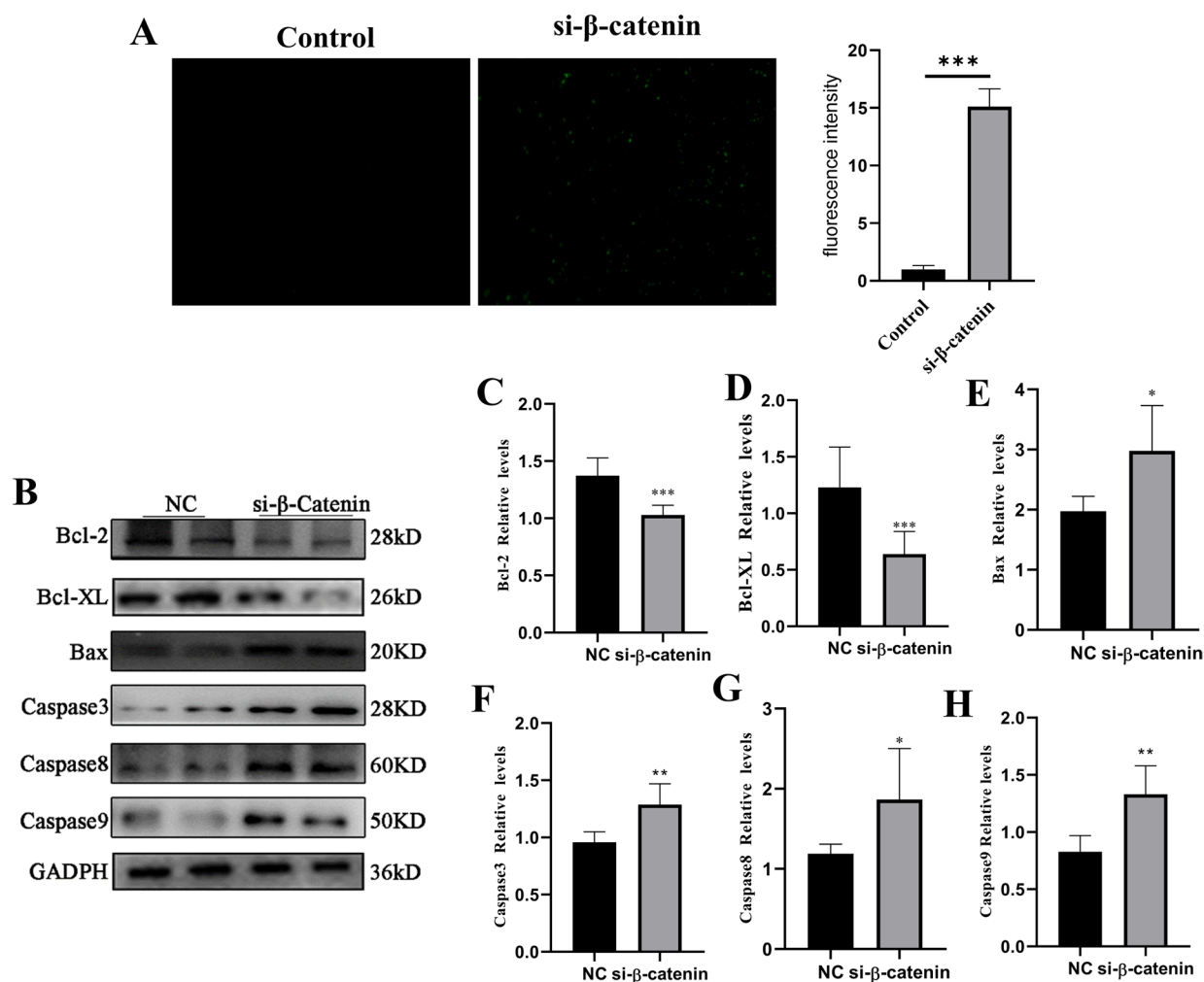


Fig. 5 Silencing β -catenin promoted apoptosis of HepG2 cells. **A** TUNEL staining measured the apoptotic rate of HepG2 cells transfected by si- β -catenin. **B** The apoptotic-related protein expression of Bcl-2, Bcl-XL, Bax, and caspase-3/8/9 was detected by Western blot-

ting in HepG2 cells transfected by si- β -catenin. **C–H** The representative column diagrams showed results of relative protein expression of Bcl-2, Bcl-XL, Bax, and caspase-3/8/9. Data was represented as the mean \pm SD of three independent experiments. ** $P < 0.01$ vs. NC

caspase-3/8/9 was upregulated. The results suggested that silencing lncRNA β -catenin promoted apoptotic of HepG2 cells.

Silencing lncRNA β -catenin induced autophagy of HepG2 cells

In addition, we examined the effect of β -catenin on the autophagy of HepG2 cells. Western blot also verified the level of β -catenin and the related level of autophagy protein in cells intervened by ICA. The results showed that si- β -catenin inhibited the expression of β -catenin and LC3-I and promoted the expression of LC3-II, Atg5, Atg7, Atg8, and Beclin-1, and ICA strengthens the role of si- β -catenin, while 3-MA promotes the role of si- β -catenin and ICA (Fig. 6). The results suggested that silencing β -catenin induced autophagy of HepG2 cells.

ICA suppressed the tumor growth in vivo

To further assess ICA's impact on hepatocellular carcinoma, we established a xenograft mouse model. ICA treatment significantly reduced the weight and volume of xenograft tumors (Fig. 7A, B). Additionally, survival analysis indicated that ICA treatment improved survival rates of the treated mice, extending survival times significantly compared to the control group (Fig. 7C). Moreover, ICA markedly decreased the expression of the proliferation marker Ki67 in xenograft tumors (Fig. 7D), aligning with our in vitro findings. ICA also reduced the expression of p62 and LC3-I, along with phosphorylation levels of PI3K, AKT, and mTOR (Fig. 8), confirming its antitumor efficacy.

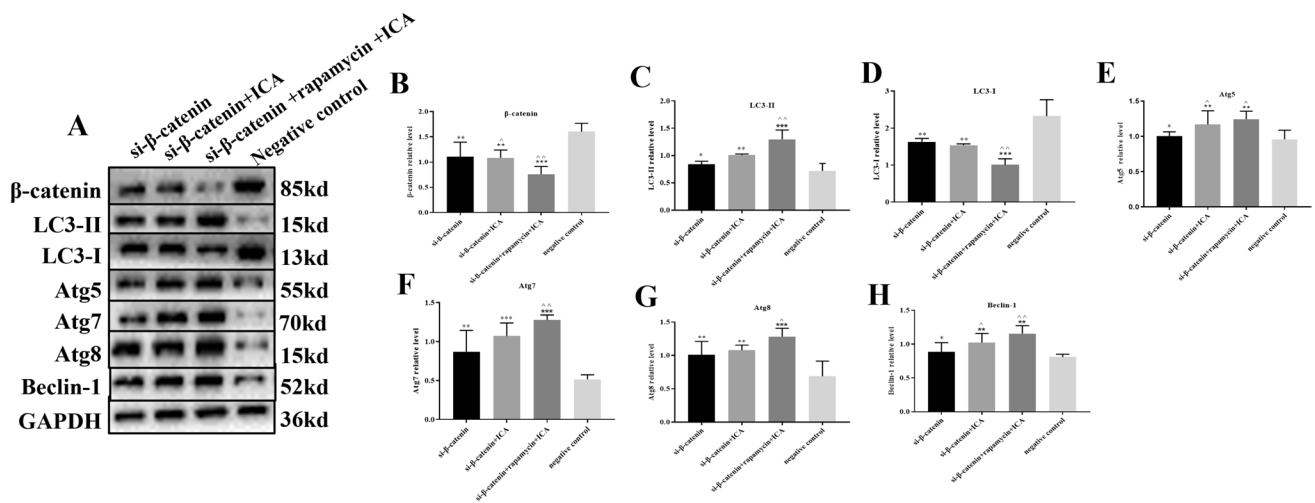


Fig. 6 Silencing β -catenin induced autophagy of HepG2 cells. **A** HepG2 cells were treated with si- β -catenin, si- β -catenin+ICA, si- β -catenin + rapamycin+ICA, and negative control. Protein expression of β -catenin, LC3-II/LC3-I, Atg5, Atg7, Atg8, and Beclin-1 was performed by Western blotting. **B–H** The representative column

diagrams showed results of relative protein expression of β -catenin, LC3-II/LC3-I, Atg5, Atg7, Atg8, and Beclin-1. Data was represented as the mean \pm SD of three independent experiments. $**P < 0.01$ vs. NC, $**P < 0.01$ vs. ICA+3-MA

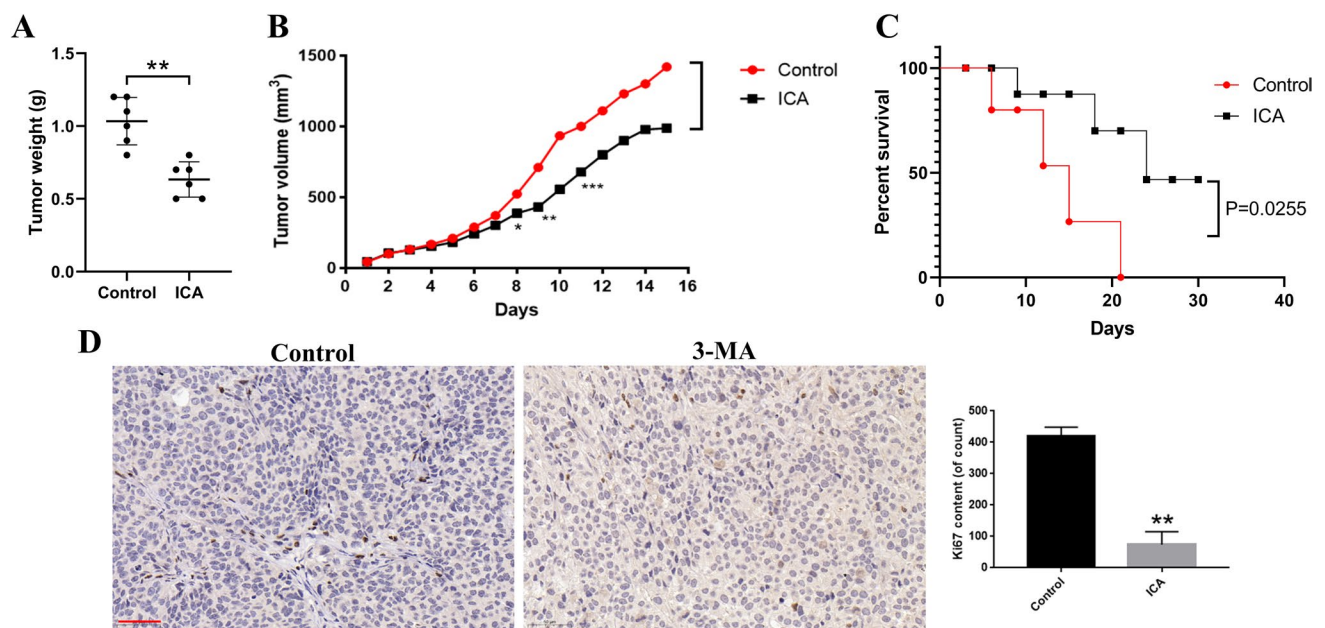


Fig. 7 ICA suppressed the tumor growth in vivo. Nude mice bearing subcutaneous xenograft HepG2 were treated with PBS, 40 mg/kg ICA alone. **A, B** The tumor weight and volume were determined when the mice were killed on the 30th day. **C** The survival of mice

was determined every 2 days for 30 days. **D** Expression of Ki67 was analyzed by immunohistochemistry (magnification, $\times 400$). $**P < 0.01$ vs. control

Discussion

ICA, a natural active ingredient in Epimedium herb (Li et al. 2021), has been identified as an inhibitor of autophagy and inducer of apoptosis in tumors (Bailly 2020; Jiang et al.

2018; Tang et al. 2015). However, its role in modulating the crosstalk between autophagy and apoptosis during anti-HCC activity remains unexplored. During HCC progression, autophagy plays a dual role, both inhibiting and promoting cancer, which may lead to completely different

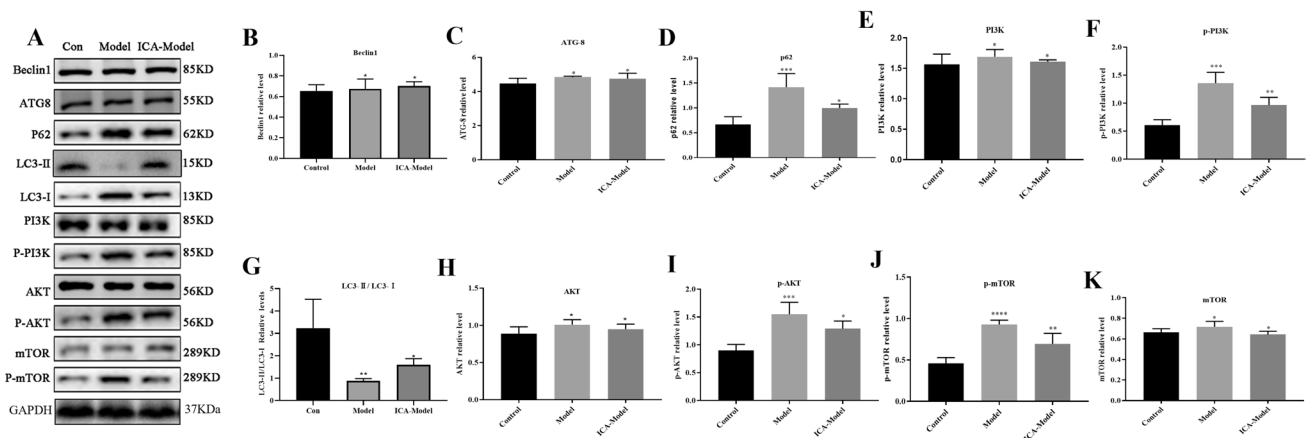


Fig. 8 ICA-induced autophagy of tumor in vivo. **A** The protein expression of autophagy-related markers (Beclin-1, ATG8, p62, LC3-II/LC3-I) and PI3K/AKT/mTOR and p-PI3K/p-AKT/p-mTOR was detected by Western blotting in tumor tissue. GAPDH was used as the control. **B–K** The representative column diagrams showed results

of relative protein expression of Beclin-1, ATG8, p62, LC3-II/LC3-I, PI3K/AKT/mTOR, and p-PI3K/p-AKT/p-mTOR. Data was represented as the mean \pm SD of three independent experiments. $^{**}P < 0.01$ vs. NC

outcomes. This phenomenon may be influenced by shared genes, such as Bcl-2 and Atg5, which regulate autophagy and apoptosis. Although autophagy and apoptosis are distinct processes, they can be initiated by common upstream signals, potentially resulting in the concurrent activation of both pathways (Sun et al. 2020). The pro-apoptotic effect of autophagy has been reported in liver diseases (Wang 2015). In this study, we verified that ICA can inhibit HCC and induce apoptosis of HCC cells in vitro and in vivo. Apoptosis and autophagy are closely related to the PI3K/AKT pathway. mTOR is an important downstream regulator of the PI3K/AKT pathway and plays an important role in protein synthesis and autophagy (Nakagawa et al. 2014). Our findings revealed that ICA can inhibit the progression of HCC by triggering the PI3K/AKT pathway. In addition, autophagy is essential for the growth of tumor cells, and the loss of autophagy can lead to DNA damage in cancer cells by inducing ROS (Deng et al. 2018). This study proved that ICA can induce autophagy of HCC cells in vivo for the first time. Moreover, we found that ICA induced autophagy in HCC cells, significantly increasing the expression of LC3-II and BECN1 while decreasing p62 expression. Icaritin has also been shown to play an anti-triple-negative breast cancer role by activating autophagy via the AMPK/mTOR/ULK1 pathway and promoting apoptosis (Zhao et al. 2024). Trybus et al. (2021) found physcion that increased the number of autophagic vacuoles and lysosomes, upregulated LC3 protein, and promoted cell apoptosis by activating caspase-3/7 and downregulating Bcl-2 expression, underscoring its anti-tumor efficacy. The anti-tumor mechanism of crosstalk inducing autophagy and promoting apoptosis was consistent with our results. The crosstalk between autophagy and apoptosis is manifested in the regulation of common pathways shared

by regulatory genes, including p53, Atg5, and Bcl-2, which affect cell fate. However, the mechanisms of autophagy and apoptosis in HCC need further exploration.

HepG2 cell lines, utilized extensively due to their key hepatocyte characteristics, remain popular for studying hepatic tumors. More than 40 hepatic tumor cell lines are used in research, with HepG2 being prominent for over four to five decades (Arzumanyan et al. 2021). Despite its popularity, HepG2 cells lack several uptake transporters and enzymes and the biomarker hGSTP1 for HCC (Choi et al. 2015). In this study, we used 2 cell lines, HepG2 cells and Bel-7402 cells, to explore the effects of ICA in experiments of cell proliferation, invasion, and cell apoptosis assays to avoid potential mistakes.

LOXLI-AS1 has been shown to be involved in tumor initiation and progression, but there is little data support for *LOXLI-AS1* in HCC research. Yu and Dai (2021) verified that high *LOXLI-AS1* expression predicted poor prognosis in patients with HCC, suggesting that the *LOXLI-AS1*/miR-377-3p/NFIB axis may exacerbate liver cancer progression. Overexpression of *LOXLI-AS1* in HCC cell lines was shown to promote proliferation and inhibit senescence in primary HCC cells by activating the AKT pathway, sequestering miR-1224-5p, and upregulating *ITPRIPL2* (Chen et al. 2023). This study confirmed that the expression level of *LOXLI-AS1* in hepatoma cells was significantly higher than that of L-02 cells. Meanwhile, we previously found that O-GlcNAc-mediated β -catenin glycosylation induced proliferation and invasion, inhibiting HCC cell apoptosis (Gao et al. 2019). Other studies have shown that β -catenin can reduce autophagy and increase apoptosis of tumor cells as well (Huang et al. 2020a, b). In this study, we confirmed that ICA promoted HCC cell apoptosis via

the *LOXL1-AS1*/β-catenin axis, with β-catenin reducing the expression of anti-apoptotic proteins Bcl-2 and Bcl-XL, and increasing pro-apoptotic factors Bax and caspase-3/8/9. In addition, we verified the expression of β-catenin in si-*LOXL1-AS1* HCC cells, and si-β-catenin inhibited the expression of β-catenin and LC3-I and promoted the expression of LC3-II, Atg5, Atg7, Atg8, and Beclin-1. Yu et al. (2019) found that lncRNA AWPPH promoted the proliferation, migration, and invasion of ovarian cancer cells by activating the Wnt/β-catenin signaling pathway. However, the regulatory role of the *LOXL1-AS1*/β-catenin axis in tumors remains underexplored.

Despite significant finding, our study has certain limitations as well. Our study used HepG2 cells, which, while commonly employed in HCC research, are originally derived from a benign hepatoma and may not fully represent the malignant properties of hepatocellular carcinoma. This difference, as discussed in recent literature (Arzumanyan et al. 2021), highlights the need for careful interpretation of our results.

In conclusion, this study is the first to propose and confirm that ICA can induce HCC autophagy and prompt apoptosis through the *LOXL1-AS1*/β-catenin axis, offering potential new directions for clinical treatment. However, the deeper mechanism of the effect of ICA on autophagy in liver cancer still needs to be further revealed. Therefore, examining the pathway proteins involved in ICA's effects on autophagy represents a valuable future research avenue.

Acknowledgements We are indebted to all individuals who participated in or helped with this research project. Special thanks to Shanghai Municipal Health Commission Shanghai Municipal Administrator of Traditional Chinese Medicine (No. 2020JQ005), National Natural Science Foundation of China (No. 82305334), Preclinical study of a new Chinese herbal medicine for the treatment of ascites liver cirrhosis (Spleen and Kidney Yang-deficiency Type) with the clinical formula of Qiguixiaogu cataplasma (No. 23S21900100), and Construction of Special Disease Alliance of Traditional Chinese Medicine in East China Area and Municipal Level, Shanghai Special Disease Alliance of Traditional Chinese Medicine for Liver Cirrhosis Ascites (Water Sickness) for Jun-feng Zhu for financial support.

Author contributions Gang Zhao, Jun-feng Zhu and Wan-yi Zhang conceived and designed the experiments. Si-cheng Gao were responsible for the writing and overall progress of the article. Jiu-hua Dai and Wei-ye Hu performed the experiments. Yong-yun Xu, Hai-lin Yang, Bai-yang ye, Qu-yang Hao and Qin-lin Tang analyzed and interpreted the results of the experiments. Moreover, the authors declare that all data were generated in-house and that no paper mill was used.

Funding This work was supported by Shanghai Municipal Health Commission Shanghai Municipal Administrator of Traditional Chinese Medicine (No. 2020JQ005), National Natural Science Foundation of China (No. 82305334), Preclinical study of a new Chinese herbal medicine for the treatment of ascites liver cirrhosis (Spleen and Kidney Yang-deficiency Type) with the clinical formula of Qiguixiaogu cataplasma (No. 23S21900100), and Construction of Special Disease Alliance of Traditional Chinese Medicine in East China Area and

Municipal Level, Shanghai Special Disease Alliance of Traditional Chinese Medicine for Liver Cirrhosis Ascites (Water Sickness) for Junfeng Zhu.

Data availability All source data for this work (or generated in this study) are available upon reasonable request.

Declarations

Human ethics and consent to participate This study was conducted in accordance with the ARRIVE guidelines. All procedures performed were in compliance with international and national guidelines for the care and use of laboratory animals. No human experiment was involved in our study.

Conflict of interest The authors declare no competing interests.

Open Access This article is licensed under a Creative Commons Attribution-NonCommercial-NoDerivatives 4.0 International License, which permits any non-commercial use, sharing, distribution and reproduction in any medium or format, as long as you give appropriate credit to the original author(s) and the source, provide a link to the Creative Commons licence, and indicate if you modified the licensed material. You do not have permission under this licence to share adapted material derived from this article or parts of it. The images or other third party material in this article are included in the article's Creative Commons licence, unless indicated otherwise in a credit line to the material. If material is not included in the article's Creative Commons licence and your intended use is not permitted by statutory regulation or exceeds the permitted use, you will need to obtain permission directly from the copyright holder. To view a copy of this licence, visit <http://creativecommons.org/licenses/by-nc-nd/4.0/>.

References



- Algandaby MM, Breikaa RM, Eid BG, Neamatallah TA, Abdel-Naim AB, Ashour OM (2017) Icaritin protects against thioacetamide-induced liver fibrosis in rats: implication of anti-angiogenic and anti-autophagic properties. *Pharmacol Rep* 69:616–624. <https://doi.org/10.1016/j.pharep.2017.02.016>
- Arzumanyan VA, Kiseleva OI, Poverennaya EV (2021) The curious case of the HepG2 cell line: 40 years of expertise. *Int J Mol Sci* 22(23):13135. <https://doi.org/10.3390/ijms222313135>
- Bailly C (2020) Molecular and cellular basis of the anticancer activity of the prenylated flavonoid icaritin in hepatocellular carcinoma. *Chem Biol Interact* 325:109124. <https://doi.org/10.1016/j.cbi.2020.109124>
- Chen X, Song L, Hou Y, Li F (2019) Reactive oxygen species induced by icaritin promote DNA strand breaks and apoptosis in human cervical cancer cells. *Oncol Rep* 41:765–778. <https://doi.org/10.3892/or.2018.6864>
- Chen J, Wang F, Xu H, Xu L, Chen D, Wang J et al (2020) Long non-coding RNA SNHG1 regulates the Wnt/β-catenin and PI3K/AKT/mTOR signaling pathways via EZH2 to affect the proliferation, apoptosis, and autophagy of prostate cancer cell. *Front Oncol* 10:552907. <https://doi.org/10.3389/fonc.2020.552907>
- Chen T, Zeng S, Liu Q, Chen Y, Lu J (2023) LOXL1-AS1 promotes cell proliferation in hepatocellular carcinoma through miR-1224-5p/ITPR1L2/AKT axis. *Cell Mol Biol Noisy-le-grand* 69:45–50. <https://doi.org/10.14715/cmb/2023.69.7.8>

- Choi JM, Oh SJ, Lee SY, Im JH, Oh JM, Ryu CS, Kwak HC, Lee J-Y, Kang KW, Kim SK (2015) HepG2 cells as an in vitro model for evaluation of cytochrome P450 induction by xenobiotics. *Arch Pharm Res* 38(5):691–704. <https://doi.org/10.1007/s12272-014-0502-6>
- Cordenonsi M, Zanconato F, Azzolin L, Forcato M, Rosato A, Frasson C et al (2011) The Hippo transducer TAZ confers cancer stem cell-related traits on breast cancer cells. *Cell* 147:759–772. <https://doi.org/10.1016/j.cell.2011.09.048>
- Deng G, Zeng S, Qu Y, Luo Q, Guo C, Yin L et al (2018) BMP4 promotes hepatocellular carcinoma proliferation by autophagy activation through JNK1-mediated Bcl-2 phosphorylation. *J Exp Clin Cancer Res* 37:156. <https://doi.org/10.1186/s13046-018-0828-x>
- Ferretti AC, Hidalgo F, Tonucci FM, Almada E, Pariani A, Larocca MC et al (2019) Metformin and glucose starvation decrease the migratory ability of hepatocellular carcinoma cells: targeting AMPK activation to control migration. *Sci Rep* 9:2815. <https://doi.org/10.1038/s41598-019-39556-w>
- Gao R, Zhang R, Zhang C, Liang Y, Tang W (2018) LncRNA LOXL1-AS1 promotes the proliferation and metastasis of medulloblastoma by activating the PI3K/AKT pathway. *Anal Cell Pathol (Amst)* 2018:9275685. <https://doi.org/10.1155/2018/9275685>
- Gao S, Miao Y, Liu Y, Liu X, Fan X, Lin Y et al (2019) Reciprocal regulation between O-GlcNAcylation and β -catenin facilitates cell viability and inhibits apoptosis in liver cancer. *DNA Cell Biol* 38:286–296. <https://doi.org/10.1089/dna.2018.4447>
- Guo J, Ma Y, Peng X, Jin H, Liu J (2019) LncRNA CCAT1 promotes autophagy via regulating ATG7 by sponging miR-181 in hepatocellular carcinoma. *J Cell Biochem* 120(10):17975–17983. <https://doi.org/10.1002/jcb.29064>
- Huang G, Liang M, Liu H, Huang J, Li P, Wang C et al (2020) CircRNA hsa_circRNA_104348 promotes hepatocellular carcinoma progression through modulating miR-187-3p/RTKN2 axis and activating Wnt/ β -catenin pathway. *Cell Death Dis* 11:1065. <https://doi.org/10.1038/s41419-020-03276-1>
- Huang W, Huang F, Lei Z, Luo H (2020) LncRNA SNHG11 promotes proliferation, migration, apoptosis, and autophagy by regulating hsa-miR-184/AGO2 in HCC. *Oncotargets Ther* 13:413–421. <https://doi.org/10.2147/OTT.S237161>
- Jiang S, Chang H, Deng S, Fan D (2018) Icaritin inhibits autophagy and promotes apoptosis in SKVCR cells through mTOR signal pathway. *Cell Mol Biol Noisy-le-grand* 64:4–10
- Kazimierczyk M, Kasprowicz MK, Kasprzyk ME, Wrzesinski J (2020) Human long noncoding RNA interactome: detection, characterization and function. *Int J Mol Sci* 21:1027. <https://doi.org/10.3390/ijms21031027>
- Li J, Wu PW, Zhou Y, Dai B, Zhang PF, Zhang YH et al (2018) Rage induces hepatocellular carcinoma proliferation and sorafenib resistance by modulating autophagy. *Cell Death Dis* 9:225. <https://doi.org/10.1038/s41419-018-0329-z>
- Li GH, Yu JH, Yang B, Gong FC, Zhang KW (2019) LncRNA LOXL1-AS1 inhibited cell proliferation, migration and invasion as well as induced apoptosis in breast cancer via regulating miR-143-3p. *Eur Rev Med Pharmacol Sci* 23:10400–10409. https://doi.org/10.26355/eurrev_201912_19679
- Li ML, Zhang Y, Ma LT (2019) LncRNA HCG11 accelerates the progression of hepatocellular carcinoma via miR-26a-5p/ATG12 axis. *Eur Rev Med Pharmacol Sci* 23:10708–10720. https://doi.org/10.26355/eurrev_201912_19771
- Li W, Zhang B, Jia Y, Shi H, Wang H, Guo Q et al (2020) LncRNA LOXL1-AS1 regulates the tumorigenesis and development of lung adenocarcinoma through sponging miR-423-5p and targeting MYBL2. *Cancer Med* 9:689–699. <https://doi.org/10.1002/cam4.2641>
- Li X, Zhang W, Liang L, Duan X, Deng J, Zhou Y (2020) Natural product-derived icaritin exerts anti-glioblastoma effects by positively modulating estrogen receptor β . *Exp Ther Med* 19:2841–2850. <https://doi.org/10.3892/etm.2020.8571>
- Li H, Liu Y, Jiang W, Xue J, Cheng Y, Wang J et al (2021) Icaritin promotes apoptosis and inhibits proliferation by down-regulating AFP gene expression in hepatocellular carcinoma. *BMC Cancer* 21:318. <https://doi.org/10.1186/s12885-021-08043-9>
- Liu Z, Wei X, Zhang A, Li C, Bai J, Dong J (2016) Long non-coding RNA HNF1A-AS1 functioned as an oncogene and autophagy promoter in hepatocellular carcinoma through sponging hsa-miR-30b-5p. *Biochem Biophys Res Commun* 473:1268–1275. <https://doi.org/10.1016/j.bbrc.2016.04.054>
- Liu L, Liao JZ, He XX, Li PY (2017) The role of autophagy in hepatocellular carcinoma: friend or foe. *Oncotarget* 8:57707–57722. <https://doi.org/10.18632/oncotarget.17202>
- Mo D, Zhu H, Wang J, Hao H, Guo Y, Wang J et al (2021) Icaritin inhibits PD-L1 expression by targeting protein I κ B kinase α . *Eur J Immunol* 51:978–988. <https://doi.org/10.1002/eji.202048905>
- Nahari D, Satchi-Fainaro R, Chen M, Mitchell I, Task LB, Liu Z et al (2007) Tumor cytotoxicity and endothelial Rac inhibition induced by TNP-470 in anaplastic thyroid cancer. *Mol Cancer Ther* 6:1329–1337. <https://doi.org/10.1158/1535-7163.Mct-06-0554>
- Nakagawa A, Sullivan KD, Xue D (2014) Caspase-activated phosphoinositide binding by CNT-1 promotes apoptosis by inhibiting the AKT pathway. *Nat Struct Mol Biol* 21:1082–1090. <https://doi.org/10.1038/nsmb.2915>
- Nguyen TM, Subramanian IV, Xiao X, Ghosh G, Nguyen P, Kelekar A et al (2009) Endostatin induces autophagy in endothelial cells by modulating Beclin 1 and beta-catenin levels. *J Cell Mol Med* 13:3687–3698. <https://doi.org/10.1111/j.1582-4934.2009.00722.x>
- Ni T, Lin N, Huang X, Lu W, Sun Z, Zhang J et al (2020) Icaritin ameliorates diabetic cardiomyopathy through apelin/Sirt3 signalling to improve mitochondrial dysfunction. *Front Pharmacol* 11:256. <https://doi.org/10.3389/fphar.2020.00256>
- Niu ZS, Wang WH, Dong XN, Tian LM (2020) Role of long noncoding RNA-mediated competing endogenous RNA regulatory network in hepatocellular carcinoma. *World J Gastroenterol* 26:4240–4260. <https://doi.org/10.3748/wjg.v26.i29.4240>
- Pieńkowska N, Bartosz G, Furdak P, Sadowska-Bartosza I (2021) Delphinidin increases the sensitivity of ovarian cancer cell lines to 3-bromopyruvate. *Int J Mol Sci* 22:2. <https://doi.org/10.3390/ijms22020709>
- Qin SK, Li Q, Xu JM, Liang J, Cheng Y, Fan Y et al (2020) Icaritin-induced immunomodulatory efficacy in advanced hepatitis B virus-related hepatocellular carcinoma: Immunodynamic biomarkers and overall survival. *Cancer Sci* 111:4218–4231. <https://doi.org/10.1111/cas.14641>
- Shan Y, Li P (2019) Long intergenic non-protein coding RNA 665 regulates viability, apoptosis, and autophagy via the MiR-186-5p/ MAP4K3 axis in hepatocellular carcinoma. *Yonsei Med J* 60:842–853. <https://doi.org/10.3349/ymj.2019.60.9.842>
- Spirina LV, Avgustinovich AV, Afanas'ev SG, Cheremisinina OV, Volkov MY, Choyznzonov EL et al (2020) Molecular mechanism of resistance to chemotherapy in gastric cancers, the role of autophagy. *Curr Drug Targets* 21:713–721. <https://doi.org/10.2174/1389450120666191127113854>
- Sun Q, Li J, Li F, Li H, Bei S, Zhang X et al (2019) LncRNA LOXL1-AS1 facilitates the tumorigenesis and stemness of gastric carcinoma via regulation of miR-708-5p/USF1 pathway. *Cell Prolif* 52:e12687. <https://doi.org/10.1111/cpr.12687>
- Sun R, Zhai R, Ma C, Miao W (2020) Combination of aloin and metformin enhances the antitumor effect by inhibiting the growth and invasion and inducing apoptosis and autophagy in hepatocellular carcinoma through PI3K/AKT/mTOR pathway. *Cancer Med* 9:1141–1151. <https://doi.org/10.1002/cam4.2723>

- Tang Y, Jacobi A, Vater C, Zou L, Zou X, Stiehler M (2015) Icaritin promotes angiogenic differentiation and prevents oxidative stress-induced autophagy in endothelial progenitor cells. *Stem Cells* 33:1863–1877. <https://doi.org/10.1002/stem.2005>
- Tompkins KD, Thorburn A (2019) Regulation of apoptosis by autophagy to enhance cancer therapy. *Yale J Biol Med* 92:707–718
- Trybus W, Król T, Trybus E, Stachurska A (2021) Physcion induces potential anticancer effects in cervical cancer cells. *Cells* 10:2029. <https://doi.org/10.3390/cells10082029>
- Wang K (2014) Molecular mechanisms of hepatic apoptosis. *Cell Death Dis* 5:e996. <https://doi.org/10.1038/cddis.2013.499>
- Wang K (2015) Autophagy and apoptosis in liver injury. *Cell Cycle* 14:1631–1642. <https://doi.org/10.1080/15384101.2015.1038685>
- Wang Y, Huang T, Li H, Fu J, Ao H, Lu L et al (2020) Hydrous icaritin nanorods with excellent stability improves the in vitro and in vivo activity against breast cancer. *Drug Deliv* 27:228–237. <https://doi.org/10.1080/10717544.2020.1716877>
- Wu Y, Zhang J, Li Q (2021) Autophagy, an accomplice or antagonist of drug resistance in HCC? *Cell Death Dis* 12:266. <https://doi.org/10.1038/s41419-021-03553-7>
- Xie N, Fei X, Liu S, Liao J, Li Y (2019) LncRNA LOXL1-AS1 promotes invasion and proliferation of non-small-cell lung cancer through targeting miR-324-3p. *Am J Transl Res* 11:6403–6412
- Yang JG, Lu R, Ye XJ, Zhang J, Tan YQ, Zhou G (2017) Icaritin reduces oral squamous cell carcinoma progression via the inhibition of STAT3 signaling. *Int J Mol Sci* 18:132. <https://doi.org/10.3390/ijms18010132>
- Yang X, Xie J, Liu X, Li Z, Fang K, Zhang L et al (2019) Autophagy induction by xanthoangelol exhibits anti-metastatic activities in hepatocellular carcinoma. *Cell Biochem Funct* 37:128–138. <https://doi.org/10.1002/cbf.3374>
- Yu W, Dai Y (2021) lncRNA LOXL1-AS1 promotes liver cancer cell proliferation and migration by regulating the miR-377-3p/NFIB axis. *Oncol Lett* 22:624. <https://doi.org/10.3892/ol.2021.12885>
- Yu G, Wang W, Deng J, Dong S (2019) LncRNA AWPPH promotes the proliferation, migration and invasion of ovarian carcinoma cells via activation of the Wnt/ β -catenin signaling pathway. *Mol Med Rep* 19:3615–3621. <https://doi.org/10.3892/mmr.2019.10029>
- Yu Z, Guo J, Hu M, Gao Y, Huang L (2020) Icaritin exacerbates mitophagy and synergizes with doxorubicin to induce immunogenic cell death in hepatocellular carcinoma. *ACS Nano* 14:4816–4828. <https://doi.org/10.1021/acsnano.0c00708>
- Zhao M, Xu P, Shi W, Wang J, Wang T, Li P (2024) Icaritin exerts anti-tumor activity by inducing autophagy via AMPK/mTOR/ULK1 pathway in triple-negative breast cancer. *Cancer Cell Int* 24:74. <https://doi.org/10.1186/s12935-024-03266-9>
- Zhou C, Gu J, Zhang G, Dong D, Yang Q, Chen MB et al (2017) AMPK-autophagy inhibition sensitizes icaritin-induced anti-colorectal cancer cell activity. *Oncotarget* 8:14736–14747. <https://doi.org/10.18632/oncotarget.14718>
- Zhou Y, Chen E, Tang Y, Mao J, Shen J, Zheng X et al (2019) miR-223 overexpression inhibits doxorubicin-induced autophagy by targeting FOXO3a and reverses chemoresistance in hepatocellular carcinoma cells. *Cell Death Dis* 10:843. <https://doi.org/10.1038/s41419-019-2053-8>

Publisher's Note Springer Nature remains neutral with regard to jurisdictional claims in published maps and institutional affiliations.

Authors and Affiliations

Sicheng Gao¹ · Wanyi Zhang^{2,3} · Jinhua Dai¹ · Weiye Hu¹ · Yongyun Xu⁴ · Hailin Yang⁵ · Baiyang Ye¹ · Hao Ouyang¹ · Qinlin Tang¹ · Gang Zhao¹  · Junfeng Zhu¹ 

✉ Gang Zhao
zhaogangsh@vip.163.com

✉ Junfeng Zhu
zhujftongling@163.com

¹ Yueyang Hospital of Integrated Traditional Chinese and Western Medicine, Shanghai University of Traditional Chinese Medicine, Shanghai 200083, China

² Shanghai University of Traditional Chinese Medicine, Shanghai 200071, China

³ Shanghai Zhongshan Community Health Center of Songjiang District, Shanghai, China

⁴ Shanghai Municipal Hospital of Traditional Chinese Medicine, Shanghai University of Traditional Chinese Medicine, Shanghai 200071, China

⁵ Changzheng Hospital Affiliated to Naval Medical University, Department of Traditional Chinese Medicine, Shanghai, 200003, China